Optimization Design Analysis of Boiler Blowdown Utilization on a Rotary Coal Dryer with Drum Tilt Angle Variations

Alvin Mirzawan Tarmizi[1*], Bambang Arip Dwiyantoro[2], Aripin Gandi Marbun[1]

[1]Indonesia Power, Jl. Gatot Subroto Kav.18, Kuningan, Jakarta 12950, Indonesia
[2]Department of Mechanical Engineering, Institut Teknologi Sepuluh Nopember, Surabaya 60111, Indonesia

Abstract

Lignite coal has dominated the use of steam power plants in recent years. Despite the consequences, which cause many problems, lignite is cheap and easy to obtain. One of the problems was mitigated by reducing the moisture content using a rotary coal dryer. Coal dryer is deemed uneconomical with the current energy sources from turbine extraction steam, electric heaters, and exhaust gas using large-powered fans. The waste energy from boiler blowdown, a water-vapored fluid discharged from the boiler to maintain water and steam quality, is being conducted to improve. Blowdown investigated in a rotary coal dryer type. The compressed air absorbed the heat from the blowdown through the steam coil. The hot air mixed with the coal in the rotary drum. A rotary drum was tested with the tilt angles of 0°, 10°, 20°, 30°, 40°, 50°, 60°, 70°, 80°, and 90°. The research steps were designing, preliminary modeling, numerical analysis, prototyping, and experimental performing. The result shows that the moisture content has decreased significantly from 35.37% to 21.28%, within an angle of 10°. Based on an economic assessment, this coal dryer also proves that dried lignite coal has increased 4.9% economic value than bituminous coal.

Keywords: lignite, moisture, rotary coal dryer, blowdown, steam coil, tilt, economic, bituminous

1. Introduction

One of the improvement programs currently being developed is coal drying technology. This equipment compensates for the massive use of lignite coal. While the coal has a high moisture content above 30% and causes several problems, the coal dryer effectively reduces the moisture and increases thermal efficiency by 0.25-1.6% [1, 2].

Energy sources in the coal dryer are divided into thermal, chemical, and mechanical/thermal dewatering [3–8]. In thermal, there are CFB-LP (Circulating Fluidized Bed - Low Pressure), WT-HP (Waste Heat – High Pressure), WT-EG (Waste Heat–Exhaust Gases), CFB-EG (Circulating Fluidized Bed-Exhaust Gases) [9]. The coal dryers that have been developed are BCB (Binderless Coal Briquetting, Austria) [10], UBC (Upgrading Brown Coal, Japan) [11], WTA (Fluidized-Bed type dryer with internal steam utilization, Germany) [12].

Several studies have been conducted to improve the existing coal dryers. Moon et al. use the Disc Coal Dryer type, with experimental parameters: heating plate temperature, blade rotation, coal mass flow rate, ambient conditions, and drying position in the heating plate [13]. The result is that the higher the rotation of the blades, the faster the decrease in the moisture of the coal, with the optimal drying position being the central heating plate. The condensation gas must be removed to increase the efficiency,

Another study was conducted by Park et al. [14] using the Fluidized Bed Dryer type. With temperature and speed variables observed, the result is a decrease in moisture content up to 80 to 90%. Furthermore, Park et al. [15] continued this research by testing drying efficiencies within drying duration, drying temperature, and gas velocity factors. Results showed that the moisture content reduced from 35.94 to 5.22%wt, which increased the calorific value of coal from 4,990 to 5,800 kcal/kg with test conditions at a temperature of 150°C and gas velocity at 2 m/s. The total time to remove all moisture reached after 77 minutes. Wiji [16] also studied with a drum-screw-spray prototype; the final coal moisture reached 9.8%.

The research conducted in this paper has a different energy source. The energy utilizes waste energy from the water of boiler blowdown. The water discharges continuously after being heated in a temperature range of 160°C to maintain the water and steam quality. The Rotary Coal Dryer type, as shown in Figure 1, is implemented. While the hot air was produced by the heat exchanging process between compressed air and blowdown in the steam coil and went thoroughly to the rotary drum—the wet coal approached the rotary drum by a screw conveyor and mixed with the hot air. Numerical and experimental stud-

*Corresponding author. Email: alvinmizrawan@gmail.com

ies observed the tilt angle of the drum to determine the efficiency of the drying process. Furthermore, we calculated the drying capability of blowdown and the economic aspect.

2.   Numerical and Experimental Method

The research started with designing the preliminary models, numerical analysis, prototyping, and experimental.

2.1.   Designing the Preliminary Models

Designing the preliminary models was the initial base in building a coal dryer prototype. It consisted of four main components and functions; the steam coil, rotary drum, bag filter, and bunker. Four steam coils are connected in parallel to ensure the heat capacity of blowdown. The coal drove to the rotary drum by screw-conveyors. The rotary drum was driven by an electric motor with chain and sprocket connections. The bag filter absorbed the dust of dried coal. The dry coal was stored in the bunker. Figure 2 shows the preliminary model.

With a mass flow rate of 5 tons/h from the blowdown and an outlet pipe of 8 inches, this pipe was reduced to the steam coil with a ¾ inch pipe. Furthermore, the velocity measurement on the inlet steam coil inlet using an anemometer obtained 84.51 m/s. The hot air is calculated based on the energy balance under ideal conditions, as shown in Equation (1).

$$m_h \cdot C_{p,h} \cdot (t_{h,i} - t_{h,o}) = m_c \cdot C_{p,c} \cdot (t_{c,o} - t_{c,i}) \qquad (1)$$

where m_h is the mass flow rate of blowdown, m_c is the mass flow rate of air, $C_{p,h}$ is the specific heat of blowdown, $C_{p,c}$ is the specific heat of air, $t_{h,i}$ is the temperature inlet of the blowdown, $t_{h,o}$ is the temperature outlet of the blowdown, $t_{c,i}$ is the temperature inlet of air, and $t_{c,o}$ is the temperature outlet of air.
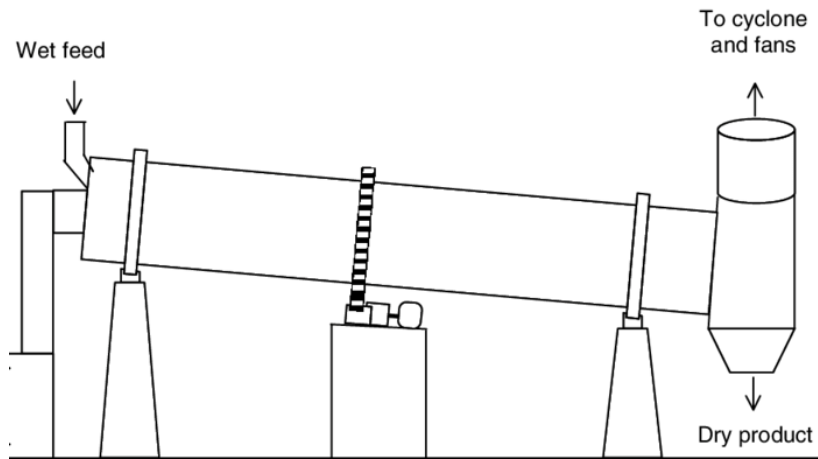

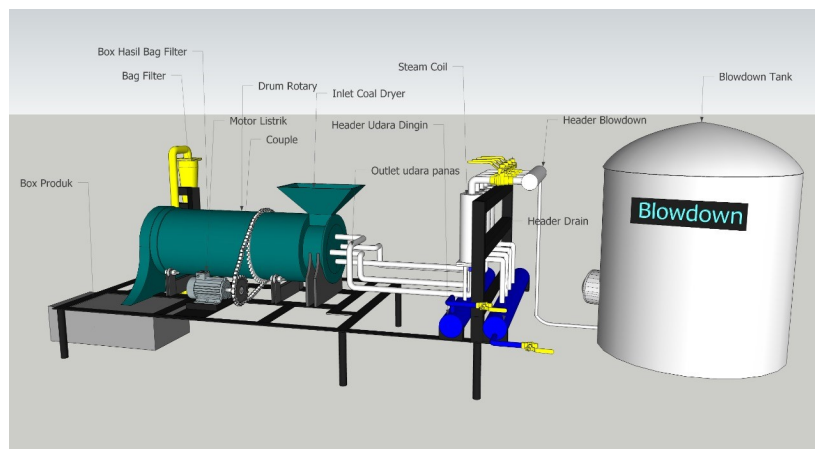**Figure 1.** Rotary coal dryer with a tilted angle.

Figure 2. Preliminary models.

2.2. Numerical Setup

Numerical calculations using a model of a single solid spherical particle without any porosity were used to resolve the particle-size effect associated with coal drying [17, 18]. The Stefan model [19] and a two-phase model [20] are often used for including the mass transfer effect of evaporated water vapor when drying a sufficiently large coal particle. However, because this study used significantly small coal particles, it was necessary to use a simplified numerical method, mainly due to a fine-sized coal particle's rapid mass and heat transfer phenomenon. Because heat transfer to a coal particle on the rotary drum could evaporate the moisture contained in the particle, it was essential to calculate the heat transfer from the hot air to the coal particle. The numerical calculation assumed that the single coal particle was spherical, and therefore, the equations used spherical coordinates.

The numerical analysis was performed with a coal particle size of 0.595 mm with a mass flow rate of 60 kg/h, and the heating temperature was set to 80 °C with a mass flow rate of 36 kg/h. The variations of the tilt angle of the rotary drum were 0°, 10°, 20°, 30°, 40°, 50°, 60°, 70°, 80°, and 90°. The domain and the grid modeling can be seen in Figure 3 and Figure 4. Several parameters such as boundary conditions, modeling, and characteristic of lignite coal are summarized in Table 1, Table 2, Table 3, and Table 4. These parameters were used to calculate the temperature and moisture content of the coal particle along with time [17]. Table 2 shows a minor difference (<1%) of the grid independence test. The mesh variations had not significantly affected the temperature changes, indicating the given mesh parameters are correct. The number of meshes used during the simulation was 1,258,654.
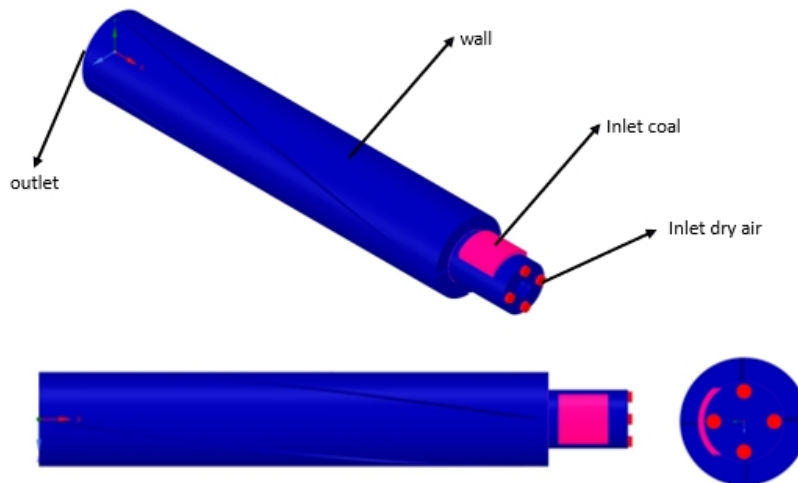

Figure 3. The domain of rotary coal dryer.

Table 1. Boundary conditions.

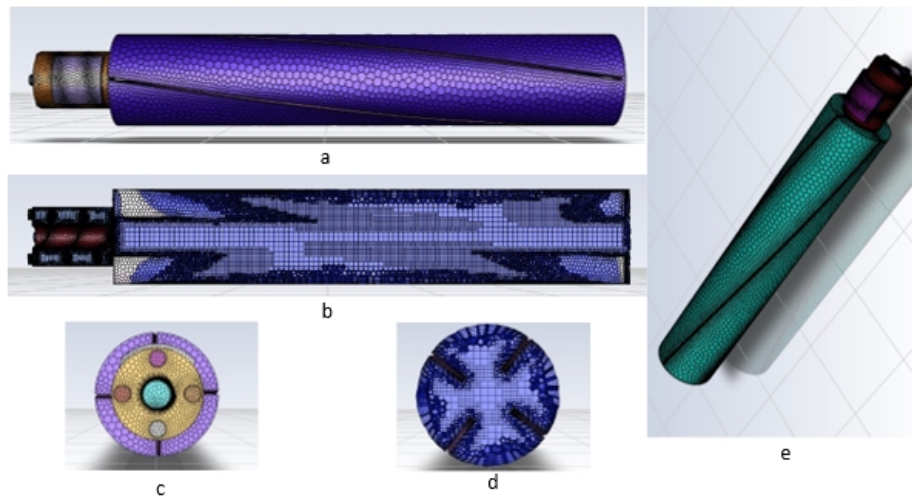| Inlet Coal		Inlet Dry Air	
Mass flow rate	60 kg/h	Mass flow rate	36 kg/h
Total temperature	30°C	Total temperature	70°C
Lv_vol	0.334	Lv_vol	0
O2	0	O2	0.21
CO2	0	CO2	0
H2O	0.3388	H2O	0
N2	0	N2	0
H2	0	H2	0
Wall.rot (rotating part)		Wall.stat (static part)	
Speed	0.733 rad/s	Thermal	Convection
Thermal	Heat flux	Heat transfer coeff.	12.12 W/m^2.°C
		Free stream temp.	26.85°C

Figure 4. Structure and grids of the rotary coal dryer model (a) Top view, (b) Top cut view, (c) Right view, (d) Right cut view, (e) Overall (3D).

Table 2. Grid independence test.

No.	Number of mesh	Temperature (℃)	Approximate error (%)
1	382,645	36.566	-
2	729,734	36.572	0.015
3	1,258,654	36.472	0.272
4	2,326,679	36.788	0.865

Table 3. Modeling parameters.

Parameter	Type
Solver	Pressure Based
Velocity Formulation	Absolute
Time	Steady
Energy	On
Viscous	Standard k-ϵ
Species	Species Transport, Finite-Rate/Eddy Dissipation
Discrete Phase	On, Coal injection
Injection Type	Surface
Particle Type	Combusting
Material	Coal mv
Diameter Distribution	Uniform
Inlet coal	Mass flow Inlet
Inlet hot air	Mass flow Inlet
Outlet	Outflow
Fin wall	Rotating wall
Tube wall	Wall, Thermal (Convection)
Pressure-Velocity Coupling Scheme	SIMPLE
Spatial Discretization Gradient	Least Squares Cell-Based
Pressure	Second Order
Momentum	Second-Order Upwind
Energy	Second-Order Upwind
Turbulent Kinetic Energy	Second-Order Upwind
Turbulent Dissipation Rate	Second-Order Upwind

Table 4. Characteristics of Indonesian lignite coal.

Parameter	Unit	Result			Method
		ARB	ADB	DAFB	
Proximate Analysis:					
- Total Moisture	%wt	35.37	-	-	ASTM D3302M-17
- Moisture in Analysis	%wt	-	13.31	-	ASTM D3173-17
- Ash Content	%wt	3.85	5.16	-	ASTM D3174-18
- Volatile Matter	%wt	-	43.45	-	ASTM D3175-17
- Fixed Carbon	%wt	-	38.08	-	ASTM D3172-13
- Total Sulphur	%wt	0.11	0.15	0.18	ASTM D4239-18
- Gross Calorific Value	kcal/kg	4,063	-	-	ASTM D5865-13
Ultimate Analysis:					
- Hydrogen	%wt	-	4.18	-	ASTM D5373-16
- Carbon	%wt	-	58.38	-	ASTM D5373-16
- Nitrogen	%wt	-	0.57	0.70	ASTM D5373-16
- Oxygen	%wt	-	18.25	-	ASTM D5373-16

2.3. Experimental Setup

Experimental was carried out with the same conditions as numerical setup. The heat exchange between blowdown at 153ºC and air compressor at 30ºC produced 80ºC temperature of drying air with a mass flow rate of 36 kg/h. The tilt of the rotary drum was set at 0º, 10º, 20º, and 30º tilt angles as it had not changed significantly based on the numerical analysis. Furthermore, pre-drying and post-drying data were conducted under international standard test methods under ISO 17025:2017 accredited laboratory.

The prototype of the coal dryer in Figure 5 was made based on the preliminary model design and numerical studies that have been carried out.
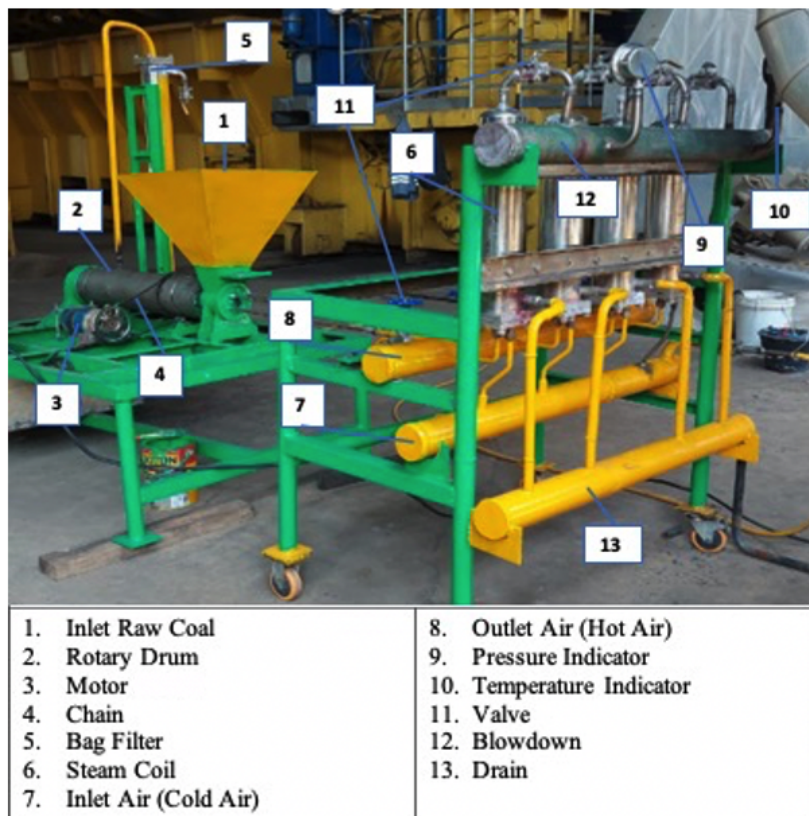

1.	Inlet Raw Coal	8.	Outlet Air (Hot Air)
2.	Rotary Drum	9.	Pressure Indicator
3.	Motor	10.	Temperature Indicator
4.	Chain	11.	Valve
5.	Bag Filter	12.	Blowdown
6.	Steam Coil	13.	Drain
7.	Inlet Air (Cold Air)		

Figure 5. The prototype of the coal dryer.

3. Results and Discussion

3.1. The Hot Air of the Dryer under Ideal Conditions

The heat energy of blowdown with the temperature, T_1, is still sufficient to meet the needs of the coal dryer, as shown in Table 5. The hot air produced, T_2, is maintained at a safe temperature to eliminate spontaneous combus- tion of the coal in the coal dryer. In Figure 6, the CFD simulation on the steam coil shows that the hot water needs are met. Figure 7 and Figure 8 show the occur- rence of spontaneous combustion at a temperature above 87ºC, where the temperature increases significantly at the beginning of the iteration.

Table 5. Heat exchange in the steam coil under ideal conditions.

No	T_2 (°C)	T_1 (°C)
1	70	146.0
2	75	145.1
3	80	144.3
4	85	143.4
5	90	142.5
6	95	141.7
7	100	140.8
8	105	139.9
9	110	139.0
10	115	138.2
11	120	137.3
12	125	136.4
13	130	135.5
14	135	134.7
15	140	133.8
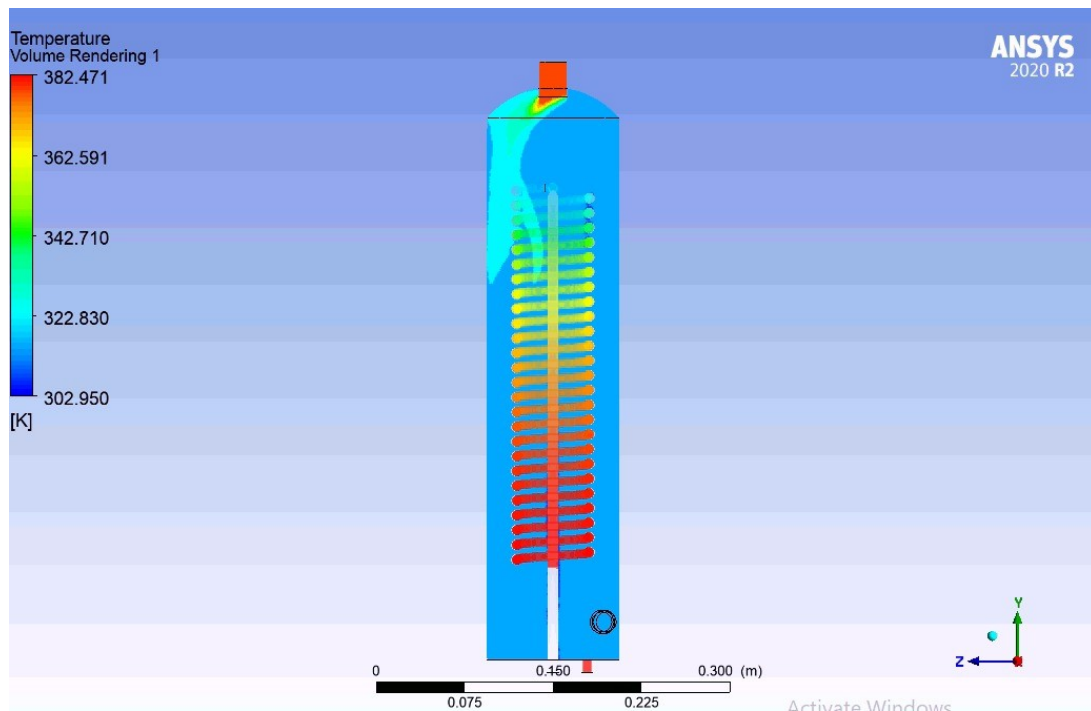
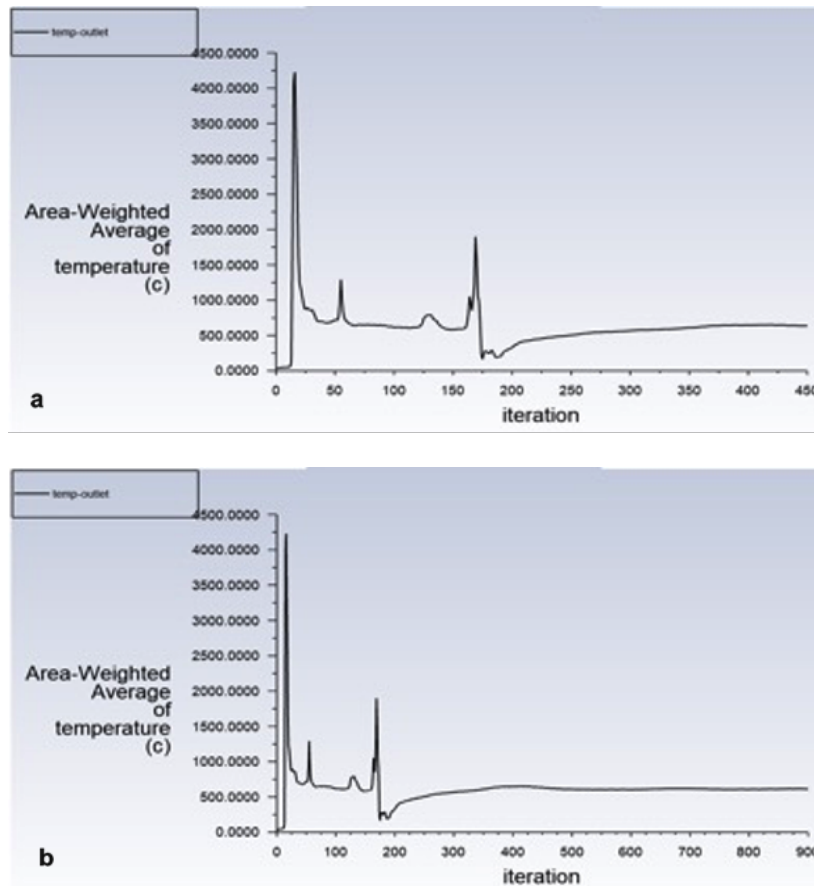**Figure 6.** Hot air CFD under ideal conditions.

Figure 7. At the beginning of the iteration, the temperature rise indicates spontaneous combustion at a temperature of (a) 88ºC, (b) 90ºC.
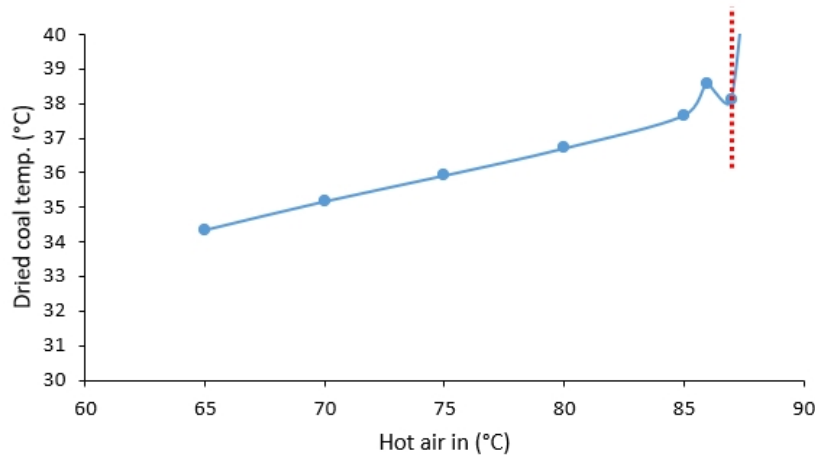

Figure 8. The hot air temperature limitation is above 87ºC.

3.2. Numerical Analysis Results

The results in Figure9 and Figure10 show a change in the coal output temperature within a different tilt angle. The higher the tilt angle, the higher the temperature was. At a temperature range of 36.4ºC to 37.6ºC, the temperature rose significantly at a tilt angle of 10º. The tilt's pitch and flight's geometry combination on the rotary drum provide the most considerable heat exchange cross-sectional area. The hot air pushes the coal and covers the coal almost along the walls in the rotary drum, affecting the increase of total heat needed, as shown in Figure11.
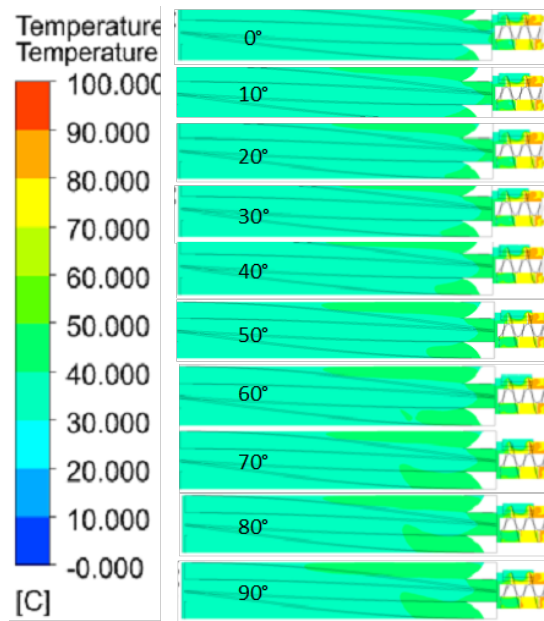
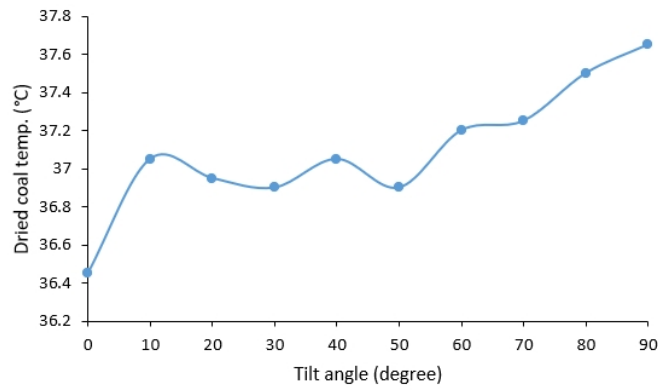**Figure 9.** Contours of coal temperature at the rotary drum.

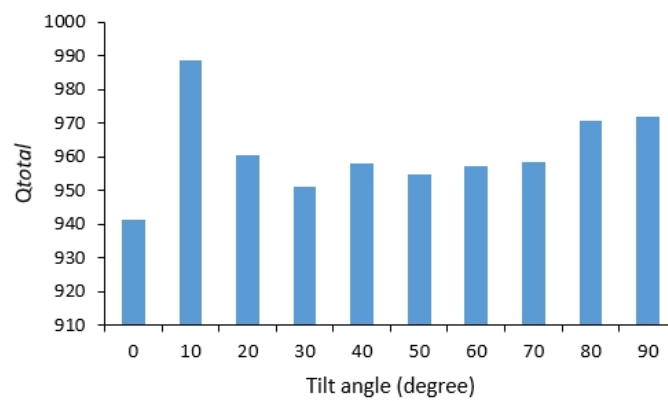**Figure 10.** Effect of tilt angle on the outlet coal temperature at rotary coal dryer.

Figure 11. The total heat needed to evaporate moisture.

Figure 12 and Figure 13 show a decrease in moisture content with a change in the tilt angle of the rotary drum. The moisture content reduction is about 13%. The most significant occurs in the tilt angle of 10°, where the rotary drum's combination of tilt angle and flight geometry provides the most considerable heat exchange cross-sectional area compared to other tilt angles. The coal and the hot air mixed well along with the rotary drum. An inhomogeneous mixing in a particular part indicates that the flight geometry does not temporarily push the coal before continuing. This process increases the residence time of coal in the rotary drum so that the moisture content of the coal decreases. The clear comparison in each tilt angle is expressed in Figure 14, while a low moisture and outlet coal temperature ratio took place at the tilt angle of 10°. This ratio also indicates the most efficient grade to absorb the heat and evaporate the moisture.
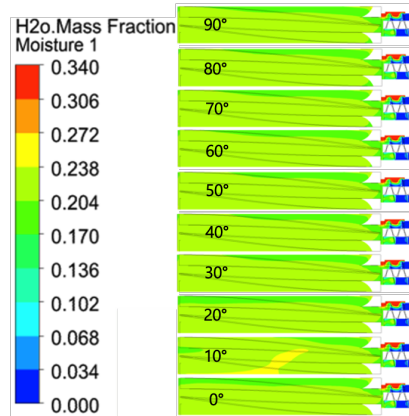
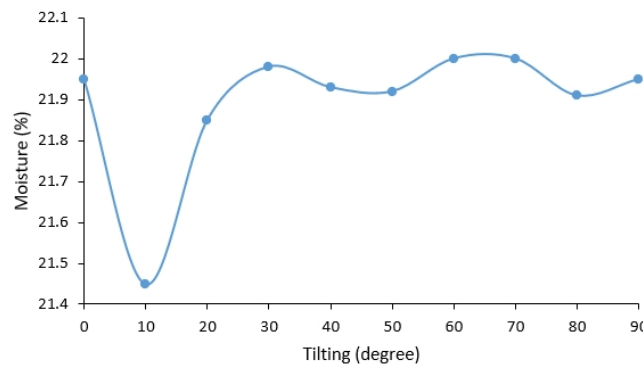**Figure 12.** Contours of H_2O mass fraction at the rotary drum.

Figure 13. Effect of tilt angle on the moisture at rotary coal dryer.
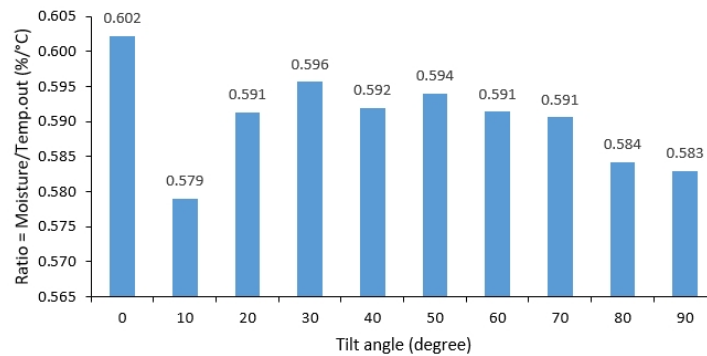
Figure 14. Dryer thermal efficiency by a ratio of moisture and outlet coal temperature.

3.3. Experimental Results

Table 6 shows a decrease in moisture content with a change in the tilt angle of the rotary drum. The most significant reduction in moisture content occurred at a tilt angle of 10º, with moisture-dried coal content of 21%. Within the same mass, the residence time at the tilt angle of 10º lasts longer, resulting in a longer drying time and triggering a better decrease in moisture content.

The decrease of moisture in coal automatically increases the gross calorific value of coal. The results are shown in Table7 and Figure 15, where the optimum tilt angle is 10º, the gross calorific value reaches 5,283 kcal/kg. The decrease in moisture content causes other compositions of coal such as C, H, O, and S to increase; by Dulong's formula, the calorific value of coal increases.

3.4. Numerical and Experimental Comparison

The result shows that within a tilt angle of 10º of the rotary drum, the coal dryer was in the top performance. It can be described in Figure 16, where the moisture content reaches 21.45% by numerical analysis and 21.28% by experimental version.

Table 6. Effect of tilt angle on the moisture content at experimental.

Tilting (°)	Mass flow rate (kg/h)	Particle size (mm)	Mass (kg)	Duration (sec)	Moisture content (%)
0	60	0.595	10	602.52	21.86
10	60	0.595	10	610.08	21.28
20	60	0.595	10	607.56	21.60
30	60	0.595	10	605.04	21.64

Table 7. Effect of tilt angle on the gross calorific value at experimental.

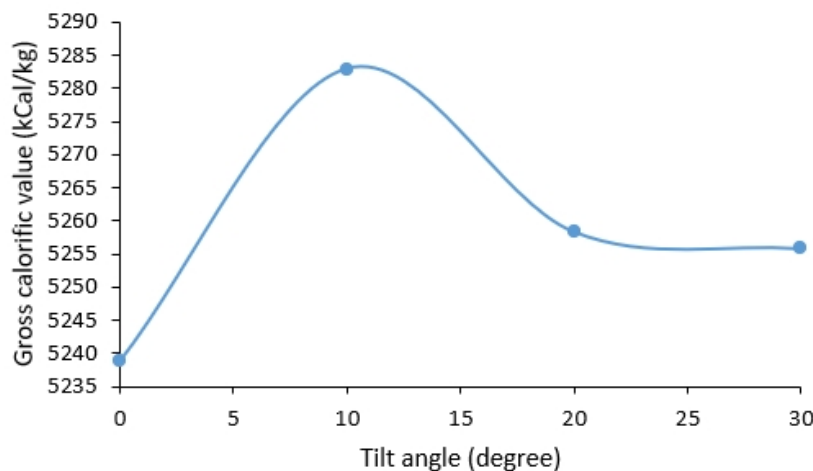| Tilting (°)	Mass flow rate (kg/h)	Particle size (mm)	Experiment (kcal/kg)			Average Gross Calorific Value (kcal/kg)
			1	2	3	
0	60	0.595	5,249	5,232	5,236	5,239
10	60	0.595	5,272	5,283	5,293	5,283
20	60	0.595	5,249	5,274	5,252	5,258
30	60	0.595	5,271	5,252	5,245	5,256

Figure 15. Effect of tilt angle on the gross calorific value of coal.
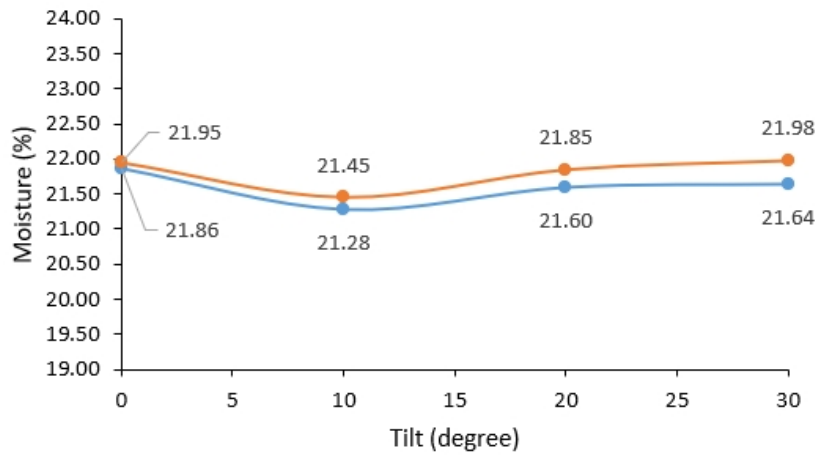
Figure 16. The comparison of numerical and experimental in a rotary coal dryer.

3.5. The Maximum Capacity of Blowdown as a Heat Source

Based on the specifications of the seven pieces of Atlas Copco type ZR110 located at the Pangkalan Susu Power Stations, Indonesia, with each capacity of 16 m³/min and power of 110 kW, the compressors can support up to 15 times of the prototype. Meanwhile, with the blowdown capacity of 5 tons/hour at a temperature range of 153°C, the prototype can be developed up to 11 times more extensively. Therefore, the rotary coal dryer prototype could be upgraded 11 times based on the passage described.

3.6. The Economic Assessment of Coal Dryer

The prices of lignite, bituminous, and dried coal can be seen in Figure 17. Dried coal, the drying version of lignite, has a 6.8% cheaper price within equal calorific value to bituminous coal. This analysis demonstrates that the production costs incurred (using electric motors, compressors, etc.), plus the coal mass lost during the drying process of lignite coal, are still profitable compared to the purchase of raw bituminous coal.

4. Conclusion

Based on the analysis that has been done, changes in the tilt angle of the rotary drum affect the optimization of the drying process in the coal dryer, with the optimal angle being 10°. This tilt angle optimization can affect the moisture content produced with an efficiency of 7%. The efficiency increase also impacts the coal prices. From an economic point of view, the use of coal dryers for lignite coal (low rank), which produces dried coal, still provides a 4.9% profit compared to raw bituminous coal (medium rank). The coal dryer can be enlarged with a capacity of up to 33 tons/day to optimize the benefits.
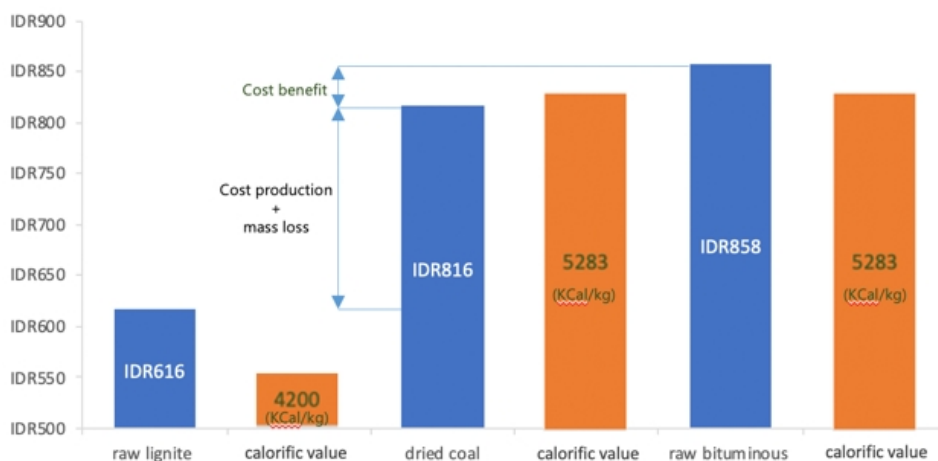
Acknowledgments

Figure 17. Coal price comparison

References

[1] M. M. Łukowicz H., Chmielniak T., "The analysis of supercritical steam power plants with a flue gas heat recovery," *Archives of Energetics*, vol. 38, no. 2, pp. 31–39, 2008.

[2] M. Pronobis, "Modernization of steam generators," in *WNT Warszawa*, pp. 197–207, 2002.

[3] R. A. Wheeler, A. F. A. Hoadley, and S. Clayton, "Modelling the mechanical thermal expression behaviour of lignite," *Fuel*, vol. 88, no. 9, pp. 1741–1751, 2009.

[4] C. Bergins, "Mechanical/thermal dewatering of lignite. Part 2: A rheological model for consolidation and creep process," *Fuel*, vol. 83, no. 3, pp. 267–276, 2004.

[5] C. Bergins, J. Hulston, K. Strauss, and A. L. Chaffee, "Mechanical/thermal dewatering of lignite. Part 3: Physical properties and pore structure of MTE product coals," *Fuel*, vol. 86, no. 1-2, pp. 3–16, 2007.

[6] C. Vogt, T. Wild, C. Bergins, K. Strauss, J. Hulston, and A. L. Chaffee, "Mechanical/thermal dewatering of lignite. Part 4: Physico-chemical properties and pore structure during an acid treatment within the MTE process," *Fuel*, vol. 93, pp. 433–442, 2012.

[7] C. Bergins, "Kinetics and mechanism during mechanical/thermal dewatering of lignite," *Fuel*, vol. 82, no. 4, pp. 355–364, 2003.

[8] J. Hulston, G. Favas, and A. L. Chaffee, "Physico-chemical properties of Loy Yang lignite dewatered by mechanical thermal expression," *Fuel*, vol. 84, no. 14-15, pp. 1940–1948, 2005.

[9] H. Kruczek, "Some problems of the combustion of young low-metamorphisms rank fossil fuels, monograph 33," *Ofic. Wyd. PWr*, 2003.

[10] S. Mangena, G. De Korte, R. McCrindle, and D. Morgan, "The amenability of some Witbank bituminous ultra fine coals to binderless briquetting," *Fuel Processing Technology*, vol. 85, no. 15, pp. 1647–1662, 2004.

[11] D. F. Umar, H. Usui, and B. Daulay, "Change of combustion characteristics of Indonesian low rank coal due to upgraded brown coal process," *Fuel processing technology*, vol. 87, no. 11, pp. 1007–1011, 2006.

[12] H. Klutz, C. Moser, and D. Block, "WTA fine grain drying: module for lignite-fired power plants of the future. Development and operating results of the fine grain drying plant," *VGB PowerTech*, vol. 86, 2006.

[13] S.-H. Moon, I.-S. Ryu, S.-J. Lee, and T.-I. Ohm, "Optimization of drying of low-grade coal with high moisture content using a disc dryer," *Fuel processing technology*, vol. 124, pp. 267–274, 2014.

[14] J. Park, S. Lee, J. H. Seo, D. Shun, D.-H. Bae, and J. H. Park, "The effect of gas temperature and velocity on coal drying in fluidized bed dryer," 2010.

[15] J. H. Park, C.-H. Lee, Y. C. Park, D. Shun, D.-H. Bae, and J. Park, "Drying efficiency of Indonesian lignite in a batch-circulating fluidized bed dryer," *Drying Technology*, vol. 32, no. 3, pp. 268–278, 2014.

[16] W. Mangestiono, "Pembuatan prototipe pengering batubara untuk mengurangi moisture content pada PLTU," *Gema Teknologi*, vol. 18, no. 1, pp. 46–51.

[17] M. Shin, H. Kim, D. Jang, and T. Ohm, "Novel fry-drying method for the treatment of sewage sludge," *Journal of Material Cycles and Waste Management*, vol. 13, no. 3, pp. 232–239, 2011.

[18] M. Farid and S. Butcher, "A generalized correlation for heat and mass transfer in freezing, drying, frying, and freeze drying," *Drying technology*, vol. 21, no. 2, pp. 231–247, 2003.

[19] M. Farid and S. Butcher, "A generalized correlation for heat and mass transfer in freezing, drying, frying, and freeze drying," *Drying technology*, vol. 21, no. 2, pp. 231–247, 2003.

[20] R. Lyczkowski, "Development of a mechanistic theory for drying of porous media using two-fluid, two-phase flow theory," *Tech. Rep., California Univ., Livermore (USA). Lawrence Livermore Lab.*, 1979.